



## LPS-squalene interaction on D-galactose intestinal absorption

Ma José Felices<sup>1</sup> · Sara Escusol<sup>1</sup> · Roberto Martínez-Beamonte<sup>2,3</sup> · Sonia Gascón<sup>1,3</sup> · Cristina Barranquero<sup>2,3</sup> · Cristina Sanchez-de-Diego<sup>4</sup> · Jesús Osada<sup>2,3</sup> · Ma Jesús Rodríguez-Yoldi<sup>1,3,5</sup>

Received: 23 October 2018 / Accepted: 17 April 2019 / Published online: 3 May 2019  
© University of Navarra 2019

### Abstract

The dynamic and complex interactions between enteric pathogens and the intestinal epithelium often lead to disturbances in the intestinal barrier, altered fluid, electrolyte, and nutrient transport and can produce an inflammatory response. Lipopolysaccharide (LPS) is a complex polymer forming part of the outer membrane of Gram-negative bacteria. On the other hand, squalene is a triterpene present in high levels in the extra-virgin olive oil that has beneficial effects against several diseases and it has also anti-oxidant and anti-inflammatory properties. The aim of this work was to study whether the squalene could eliminate the LPS effect on D-galactose intestinal absorption in rabbits and Caco-2 cells. The results have shown that squalene reduced the effects of LPS on sugar absorption. High LPS doses increased D-galactose uptake through via paracellular but also decreased the active sugar transport because the SGLT1 levels were diminished. However, the endotoxin effect on the paracellular way seemed to be more important than on the transcellular route. At the same time, an increased in RELM- $\beta$  expression was observed. This event could be related to inflammation and cause a decrease in SGLT1 levels. In addition, MLCK protein is also increased by LPS which could lead to an increase in sugar transport through *tight junctions*. At low doses, the LPS could inhibit SGLT1 intrinsic activity. Bioinformatic studies by docking confirm the interaction between LPS-squalene as well as occur through MLCK and SGLT-1 proteins.

**Keywords** LPS · Squalene · Intestinal absorption · SGLT1 · RELM- $\beta$  · MLCK

### Introduction

The intestinal mucosa is formed by epithelial cells that separate two media, the internal one from the external one. This epithelium establishes a barrier that on the one hand prevents the entrance of pathogens to the organism, thanks to the

immune system located in it, and on the other hand, it allows the passage of substances from the diet to the blood [32].

The intestinal absorption of these substances or nutrients involves selective permeability through 2 major routes: transepithelial/transcellular and paracellular pathways [31]. The transcellular permeability is carried out through the epithelium by specific proteins. This way is used for amino acids, sugars, short-chain fatty acids, and electrolytes [13]. The paracellular permeability is carried out between epithelial cells, and it is regulated by proteins located in the tight junctions [22].

In some cases, the imbalance or dysbiosis between the microorganisms of the intestinal mucosa can lead to an inflammation of the mucosa and therefore alter the transport of nutrients through it [6].

Lipopolysaccharide (LPS), a constituent of the cellular wall of Gram-negative bacteria, can act as endotoxin and can be responsible for septic syndrome [41]. This endotoxin and its derived cytokines are capable of modulating the intestinal tight junction (TJ) permeability by signal transduction pathway activation [2]. Thus, Nighot et al. have shown that myosin light chain kinase (MLCK) plays a central role in the LPS-

---

**Electronic supplementary material** The online version of this article (<https://doi.org/10.1007/s13105-019-00682-8>) contains supplementary material, which is available to authorized users.

---

✉ Ma Jesús Rodríguez-Yoldi  
mjrodyol@unizar.es

<sup>1</sup> Department of Pharmacology and Physiology, University of Zaragoza, 50013 Zaragoza, Spain

<sup>2</sup> Department of Biochemistry, Molecular and Cellular Biology, Veterinary Faculty, University of Zaragoza, 50013 Zaragoza, Spain

<sup>3</sup> CIBERobn (ISCIII), IIS Aragón, IA2, Zaragoza, Spain

<sup>4</sup> Department Physiological Sciences II, University of Barcelona, Barcelona, Spain

<sup>5</sup> Department of Physiology, Veterinary Faculty, University of Zaragoza, 50013 Zaragoza, Spain

induced increase in TJ permeability [23]. Likewise, the trans-cellular pathway can also be regulated by LPS and its cytokines acting on the specific proteins related to sugars and amino acids transport [42]. In this respect, previous studies in our laboratory have shown that LPS altered the intestinal absorption of D-galactose *in vivo* and *in vitro* by modifying the expression or activity of SGLT1 carrier [4]. In addition, the cytokines released by endotoxins, tumor necrosis factor alpha (TNF- $\alpha$ ), and interleukin 1 beta (IL-1 $\beta$ ) have also shown an inhibitory effect on D-galactose intestinal absorption. These effects could be related to the activation of multiple intracellular signaling cascades including the mitogen-activated protein kinase (MAPK) and nuclear factor  $\kappa$ B (NF- $\kappa$ B) signal transduction pathway [36, 37].

On the other hand, the Mediterranean diet reflects the eating habits of countries in the Mediterranean area. Olive oil may be the main health-promoting component of this diet since there is preliminary evidence that its regular consumption can reduce mortality by decreasing the risk of diseases such as cardiovascular diseases, cancer, neurodegeneration, arthritis, and several chronic diseases [25].

In this way, squalene is a triterpene present at high levels in the extra-virgin olive oil. This triterpene, together with phenolic compounds, is responsible for its stability. In addition, several studies have shown that squalene has beneficial effects against atherosclerosis as well as anti-inflammatory properties. Likewise, it is an anti-oxidant [38], which might play an important role in preventing ageing and skin pathologies. Squalene is also used as an adjuvant in vaccines and in other fields such as cancer [21].

For all this, the aim of this work was to study whether the squalene present in the diet of animals or added to cells was able to modify the effect induced by LPS on the intestinal absorption of galactose in two experimental models: rabbit jejunum and Caco-2 cells. We have used cells in order to see the effect of LPS and squalene in intestinal tissue free of nervous and/or hormonal signals which are present in the animal model. These cells differentiate into polarized monolayer such that their phenotype, morphologically and functionally, resembles that of the small intestinal epithelial cells and they develop the morphological characteristics of mature enterocytes [9].

## Materials and methods

### Materials

D-Galactose, D-mannitol, Hepes, Tris (hydroxymethyl) amino-methane, bovine serum albumin, dimethyl sulfoxide (DMSO), lipopolysaccharide from *E. coli* (LPS) serotype 0111:B4, squalene, and anti-actin antibody were obtained from Sigma (Spain). D-[U-14C] galactose and Biodegradable Counting Liquid

Scintillation were obtained from GE Healthcare Life Sciences. The membrane filters were provided by Millipore. The reagents used in western blot analysis were obtained from Bio-Rad, Sigma, and Serva (Spain). The cell culture material was obtained from Life Technologies (Spain).

### Animals, diets, and preparation of intestinal tissue

The experimental animals were housed, handled, and euthanized according to the European Union Legislation 86/609/EEC. All experimental protocols were approved by the Ethical Committee of the University of Zaragoza (PI47/10).

For 4 weeks, two groups of six male New Zealand rabbits were fed with a chow diet enriched with 1% of sunflower oil for the control group, and with 1% of sunflower oil and 0.5% of squalene for the squalene group. The diet supplementation in 1% of sunflower oil is required to transmit efficiently the squalene added in a 0.5%. In addition, this oil does not have the presence of other active compounds such as  $\beta$ -carotene, sterols, triterpenes, and squalene present in olive oil. The squalene amount was equivalent to a diet with 50% of caloric total intake coming from extra-virgin olive oil. After 4 weeks, the rabbits were treated with LPS using two different regimens of administration: acute (intravenous administration (IV) of LPS through the lateral ear vein, 90 mins prior to the sample collection) and chronic (the endotoxin was released for 1 week by intraperitoneal (IP) osmotic pump implantations) treatments. The animals, then, were divided into four groups: control with/without LPS and squalene with/without LPS. During the treatment, the solid intake, body weight, and rectal temperature of the animals were monitored.

Rabbits were euthanized following previously published protocols [4]. Intestinal samples were then taken and the proximal jejunum was removed and rinsed with ice-cold Ringer's solution which contained (in mM): 140 NaCl, 10 KHCO<sub>3</sub>, 0.4 KH<sub>2</sub>PO<sub>4</sub>, 2.4 K<sub>2</sub>HPO<sub>4</sub>, 1.2 CaCl<sub>2</sub>, 1.2 MgCl<sub>2</sub>, and pH 7.4.

### Sugar uptake measurements in rabbit jejunum

**Tissue uptake** Rings of everted jejunum weighing about 100 mg were continuously bubbled with 95% O<sub>2</sub>-5% CO<sub>2</sub>. Tissue rings were incubated for 3 mins in Ringer's solution at 37 °C containing 0.01  $\mu$ Ci/mL D-[U-14C] galactose plus 0.5 mM unlabeled substrate. After incubation, tissue pieces were washed and weighed as described by Amador et al. [4]. The incubation time of tissue with galactose was 3 mins. The measurements were expressed as micromole of D-galactose per gram of tissue.

**Cell culture** The Caco-2 cell line PD7 clone was kindly provided by Dr. Edith Brot-Laroche (Université Pierre et Marie Curie-Paris 6, UMR S 872, Les Cordeliers France). The

maintenance and growth of the cells were carried out following the protocol previously published [37].

For cell treatment studies, cells were seeded in 24-well plates at a density of  $4 \times 10^4$  cells/well. The culture medium (without FBS) contained LPS at concentrations of 50 and 75  $\mu\text{g}/\text{mL}$  and/or 50  $\mu\text{M}$  squalene [16]. Once the cells were treated with LPS and/or squalene for 24 h, cold and labeled D-galactose medium was added for 15 mins. The samples taken from the medium and from the cells were measured by radioactive counting.

**Determination of cytotoxicity: MTT assay** Cell proliferation inhibition was measured using the MTT [33]. Following appropriate incubation of cells, with or without LPS and/or squalene, MTT was added to each well. The incubation was continued at 37 °C for 3 h; medium was then removed by inversion and 100  $\mu\text{L}$  of DMSO per well was added. In the end, absorbance was measured with a scanning multi-well spectrophotometer at a wavelength of 560/670 nm.

**Galactose uptake in Caco-2 cells** The medium used as buffer contained 0.5 mM D-galactose with 0.01  $\mu\text{Ci}/\text{mL}$  D-[U-14C] galactose. After a pre-incubation time, the cells were incubated for 15 mins at 37 °C. The uptake was stopped with an ice-cold free-substrate buffer with 50 mM D-galactose followed by aspiration as described by Viñuales et al. [37]. Data were expressed as micromole of D-galactose per milligram protein.

**Western blotting in BBMV and homogenate** In the study with animals, brush border membrane vesicles (BBMVs) and homogenates were prepared from rabbit jejunum using the  $\text{Mg}^{2+}$  EGTA precipitation method [37] for each experimental group. Protein content was measured with the Bradford method using bovine serum albumin as standard.

Cells grown on 75  $\text{cm}^2$  plastic flasks were incubated for 24 h, in presence or absence of LPS and/or squalene. After the incubation period, BBMVs and homogenates were isolated [10]. A phosphatase inhibitor cocktail B (Santa Cruz Biotechnology sc-45045) was used in cell extracts (BBMV and homogenate). The protein content was determined by the Bradford method.

The same amounts of vesicles and homogenates protein (20  $\mu\text{g}$ ) from controlled and treated animals or cells were solubilized in the buffer and resolved as described by Viñuales et al. [37]. The following primary antibodies were used: rabbit polyclonal anti-SLC5A1 (SGLT1) (Abnova, H00006523-D01P), anti-rabbit polyclonal RELM beta (Biorbyt, orb100867), and human monoclonal anti-MLCK (Millipore, MABT194). The following secondary antibodies coupled to peroxidase were used: goat anti-mouse (Millipore AP200P) and rabbit anti-goat (Sigma A5420). Membranes were exposed to autoradiography film, Blue UltraCruz (Santa Cruz Biotechnology) for several time periods to achieve signal intensity within the dynamic range of quantitative detection. Films were scanned at a 600-dpi resolution (via

AGFA Arcus II). The intensity of bands for each condition was calculated using Quantity One software version 4.5.0 (BioRad).

**Protein modeling** The sequences of rabbit SGLT1 and MLCK were retrieved from Uniprot (<http://www.uniprot.org/>) entries P11170 and P29294 respectively and submitted to the online server Robetta for structure modeling (<http://rosetta.bakerlab.org/>) [30]. Robetta provides both ab initio and comparative models of protein domains. Firstly, protein chains were parsed into putative domains and aligned with template PDBs. Domains without a detectable PDB homolog were modeled with the Rosetta de novo protocol [29]. Alignments were clustered and comparative models were generated using the RosettaCM protocol [30]. Obtained structures were validated using ProSA-web (<https://prosa.services.came.sbg.ac.at/prosa.php>) [40] and ModEval (<https://modbase.compbio.ucsf.edu/evaluation/>). MOEval was run using MatchBySS training set. Ramachandran plot was assessed using RAMPAGE.

**Docking** For SGLT1, the docking step was performed using the molecular docking program SwissDock web service (<http://www.swissdock.ch/>) which uses calculations performed in the CHARMM force field with EADock DSS24 [15]. The ligand and receptor files in the appropriate formats were uploaded to the web-based server for docking study. For the receptor, we used the obtained PDB from the protein modeling step. Ligand files were obtained from Zinc database (<http://zinc.docking.org/>). The structures of the ligands used were ZINC06845904 for squalene and ZINC38377593 for lipopolysaccharide. Docking was performed using the “accurate” parameter with no region of interest defined (blind docking approach). Flexibility for side chains was set at 0 Å within of any atom of the ligand in its reference binding. Simultaneously, CHARMM energies of the interactions were estimated on the grid [15]. Results were downloaded and visualized in the UCSF Chimera package (<http://www.rbvi.ucsf.edu/chimera>) [24].

Since the docking step for MLCK was not supported by Swissdock due to the large size of the protein, RosettaLigand server was used for protein-ligand docking with MLCK ([http://rosie.rosettacommons.org/ligand\\_docking](http://rosie.rosettacommons.org/ligand_docking)) [12]. RosettaLigand uses Monte Carlo minimization algorithms to model the rigid body position and orientation of the ligand as well as side-chain conformations of the protein. Then, ensembles of ligand conformations and protein backbones were used to model conformational flexibility. Finally, the models produced are evaluated with a scoring function that includes an electrostatics model, an explicit orientation-dependent hydrogen bonding potential, an implicit solvation model, and van der Waals interactions. Docking experiments were run in triplicate and only clusters with conserved positions in all the experiments were considered for further analysis.

**Statistical analysis** The results were expressed as means  $\pm$  SE. The comparison between means was performed using a one-way analysis of variance (ANOVA). Significant differences at  $p < 0.05$  were compared using Bonferroni's multiple and Mann-Whitney two-tailed comparison tests. The statistical analysis and the graphics were performed using the GraphPad Prism version 5.02 program on a PC computer.

## Results and discussion

Infections caused by Gram-negative bacteria generally involve alterations in gastrointestinal function. LPS produces, among other effects, alterations in intestinal transport. In this sense, its effect on the transport of water and electrolytes has been studied in various animal species [17]. In relation to the absorption of nutrients, it has been shown that LPS alters the absorption of sugars such as D-galactose [4].

On the other hand, preclinical studies have shown that extra-virgin olive oil, typical oil of the Mediterranean diet, has anti-inflammatory, anti-proliferative, and anti-apoptotic effects. The beneficial effects of this oil have been attributed to unsaturated fatty acids present in the majority fraction of olive oil. However, the oil contains minor components, with important biological properties, which are included in the unsaponifiable fraction extracted with solvents after saponification of the oil. Squalene is the main unsaponifiable compound and is considered one of the most relevant due to its potential preventive actions against cancer, anti-oxidant, atherosclerosis, and skin pathologies [21].

Some studies have shown that a diet rich in unsaponifiable components of olive oil reduces the damage caused by acute colitis and inhibits the inflammatory response to LPS [27]. In this sense, the anti-inflammatory effect of squalene has been demonstrated by reducing the intracellular levels of inflammatory enzymes and cytokines in neutrophils, monocytes and mouse, and human macrophages and in acute colitis in mice [7].

Therefore, the objective of this work was to study whether a diet rich in squalene in animals or the addition to intestinal cells of the triterpene could modify the effect of LPS in relation to the intestinal absorption of D-galactose.

### Animal model

#### Functional studies

After 4-week administration, the diet enriched in squalene did not modify the food intake, neither the weight of the animals (data not shown). The LPS produced an increase in the body temperature of the animals, being this effect diminished, in part, by the squalene in the diet (Figs. 1 and 2). This event could be due to the existence of possible interaction of squalene with LPS, perhaps

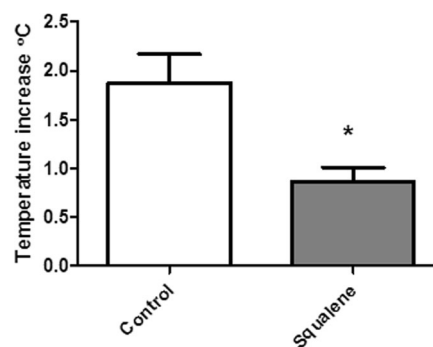


**Fig. 1** Temperature increase of rabbit treated with 6  $\mu\text{g}/\text{kg}$  bw LPS for 90 mins. Control: animals without squalene diet. Squalene: animals with squalene diet. \* $p < 0.05$  with respect to control animals

through the proteins involved in prostaglandin metabolism as it has been shown in the literature [27].

#### D-Galactose intestinal absorption

Previous studies in our laboratory have shown an inhibitory effect of LPS (2  $\mu\text{g}/\text{kg}$  bw) on intestinal absorption of D-galactose [4]. In the present report, intravenous administration of a dose three times higher of LPS (6  $\mu\text{g}/\text{kg}$  bw for 90 mins) or the chronic treatment (1 mg/kg bw for a week) produced an increase in intestinal absorption of D-galactose. This effect was not observed in the group fed the squalene diet and treated with LPS (Figs. 3a and 4a).

#### Studies of protein expression

It is well known that sugars are transported through the brush border by transport systems  $\text{Na}^+$  independent and  $\text{Na}^+$  dependent, the latter being electrogenic. D-Glucose in the lumen stimulates the synthesis of SGLT1 in the small intestine cells of rats and humans through a cascade of intracellular events, which allow the insertion of functional SGLT1 proteins into the brush border membrane of the enterocytes [28]. On the

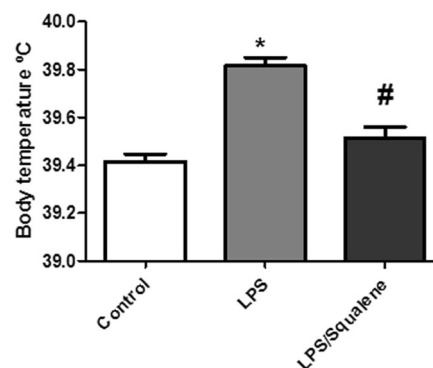


**Fig. 2** Body temperature of rabbit fed with/without squalene and treated with 1 mg/kg bw LPS for 1 week. Control: animals without squalene diet. LPS: animals without squalene diet and treated with LPS. LPS/squalene: animals with squalene diet and treated with LPS. \* $p < 0.05$  with respect to control animals. # $p < 0.05$  with respect to LPS animals

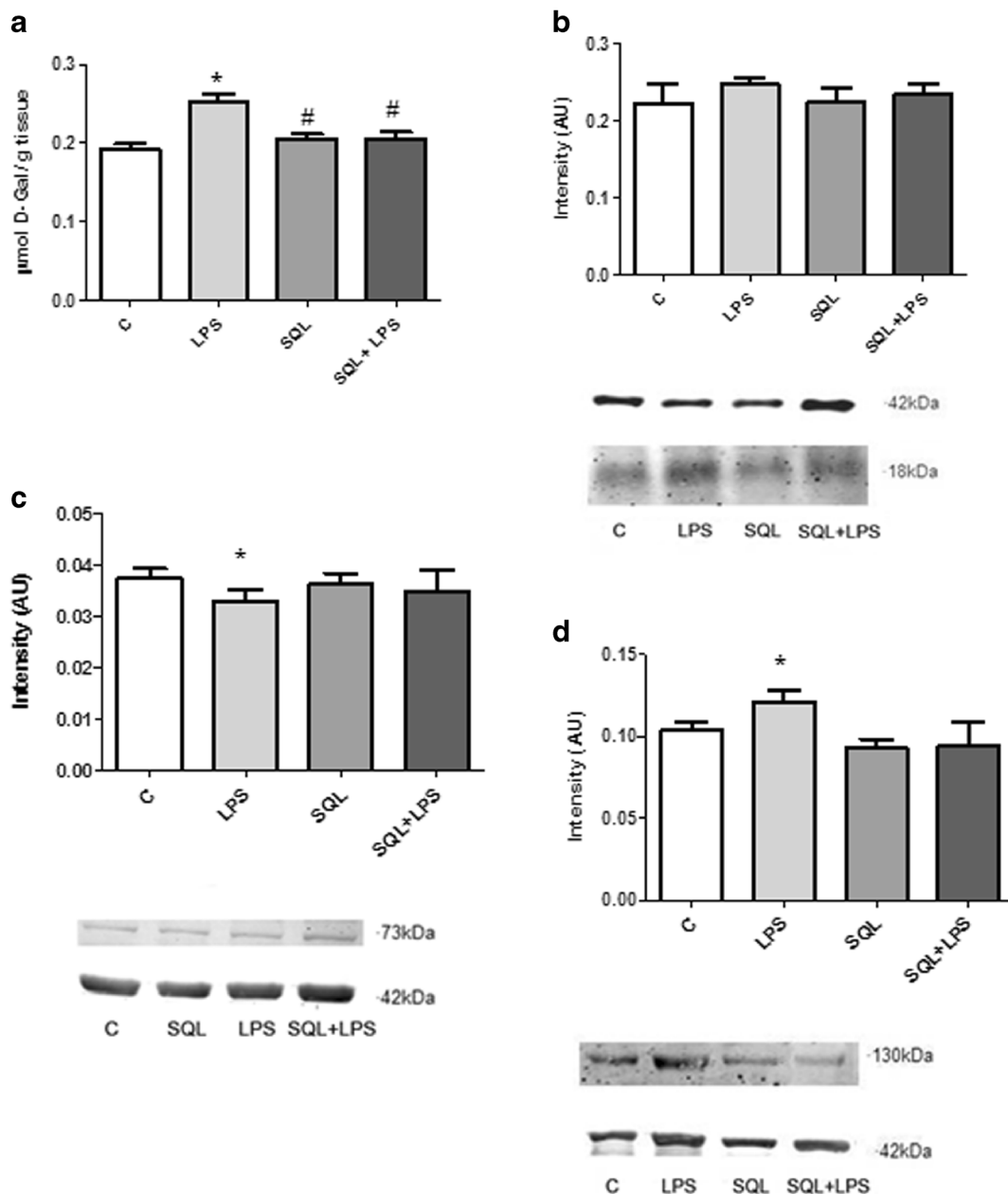


**Fig. 3** Absorption of D-galactose in the acute LPS effect. **a** Effect of the administration of LPS 6 µg/kg bw on intestinal absorption of 0.5 mM D-galactose in rabbits with control diet or diet with a squalene (SQL) supplement. The incubation time was 3 mins. The results were obtained from 6 animals per condition with 12 determinations per animal. \* $p < 0.05$  with

respect to control animals. # $p < 0.05$  with respect to LPS animals. *Protein study by western blot.* The information is given as protein expression intensity (mean  $\pm$  SEM) in arbitrary units (AU) normalized with its actin. **b** SGLT1 expression. **c** RELM- $\beta$  expression. **d** MLCK expression. \* $p < 0.05$  with respect to control animals

other hand, the decrease in sugar levels in the lumen reduced the levels of SGLT1 [34].

To determine whether the transport system (s) is influenced by the LPS, we measured the expression of the Na<sup>+</sup>-dependent protein SGLT1 by western blot. Na<sup>+</sup>-independent transport is carried out through the GLUT-2 transporter, which is blocked by phloretin and cytochalasin B [11]. This transporter can be expressed in the brush border membrane under certain circumstances, but previous studies carried out by our group have

shown that it was not expressed in our experimental conditions [14].

In the present study, significant differences in the expression of the SGLT1 protein were observed in the different groups of animals (Figs. 3b and 4b). LPS decreased the protein levels of SGLT1 and this effect was reversed in animals fed squalene.

At the same time, we observed an increased in the resistin-like molecule- $\beta$  (RELM- $\beta$ ) protein expression. This increase was only significant in the case of the acute treatment of

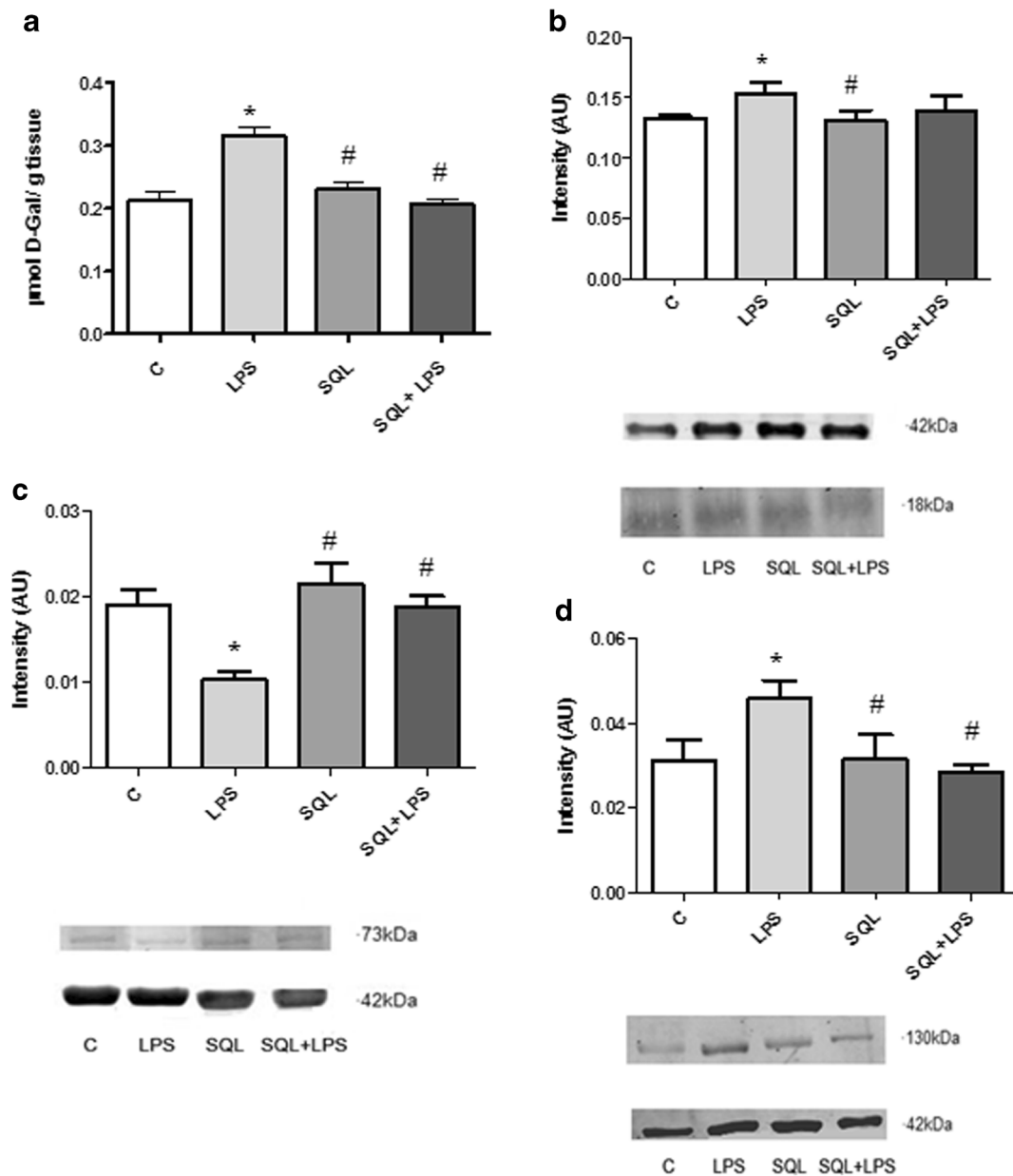


**Fig. 4** Absorption of D-galactose in the chronic LPS effect. **a** Effect of the administration of LPS 1 mg/kg bw on intestinal absorption of 0.5 mM D-galactose in rabbits with control diet or diet with a squalene (SQL) supplement. The incubation time was 3 mins. The results were obtained from 6 animals per condition with 12 determinations per animal. \* $p < 0.05$  with respect to control animals. # $p < 0.05$  with respect to LPS animals. Protein

study by western blot. The information is given as protein expression intensity (mean  $\pm$  SEM) in arbitrary units (AU) normalized to actin. **b** SGLT1 expression. **c** RELM- $\beta$  expression. **d** MLCK expression. \* $p < 0.05$  with respect to control animals. # $p < 0.05$  with respect to LPS animals

rabbits with LPS (Fig. 4c). The family of RELM- $\beta$  proteins is involved in insulin resistance, diabetes, and inflammatory processes. In addition, it reduces the activity and quantity of the SGLT1 transporter [20, 35].

Likewise, we have seen that the absorption of D-galactose was increased in LPS-treated animals which could indicate a change in the permeability of the paracellular pathways by the action of endotoxins. In this sense, several works, in vitro and in vivo, have shown that LPS increases permeability through narrow junctions [16].

Therefore, we found interesting to determine the amount of the myosin light chain kinase (MLCK) located at the periphery of the actin-myosin ring and related to changes in membrane permeability. Several studies have shown that an increase in this protein produces a greater permeability in Caco-2 cells and that it is related to sodium-dependent nutrient transporters [8]. We found a significant increase in MLCK protein in the groups of animals treated with LPS (Fig. 3d and 4d) which could justify the greater intestinal absorption of sugar found (Figs. 3a and 4a). In this case, the LPS effect was also reversed by the squalene present in the diet.

### Cell model (Caco-2 cells in culture)

In addition to using the rabbit as an experimental model, human colon adenocarcinoma cells (Caco-2) were treated to confirm the effects of LPS and squalene in a model free of nervous and/or hormonal influences.

Initially, we found interesting to determine the possible toxicity of LPS and squalene on Caco-2 cells. For this, cell viability studies were performed with the MTT technique and the cells were treated with/without 50  $\mu$ M squalene and/or LPS 50 and 75  $\mu$ g/mL for 24 h. The results have shown that LPS and squalene did not affect cell viability, at the tested concentrations, as shown in Fig. 5.

Then, we studied 0.5 mM D-galactose uptake in treated cells with LPS and/or squalene for 24 h following 15-min incubation with the sugar. The results have shown that the absorption of D-galactose was increased or decreased depending on the concentration of LPS assayed (Fig. 6a). Concentrations lower than 50  $\mu$ g/mL produced no effect on sugar transport (data not shown). However, a concentration of LPS 50  $\mu$ g/mL caused a decrease in intestinal absorption while a higher concentration of LPS (75  $\mu$ g/mL) increased the sugar absorption (Fig. 6a). This dose in parallel the increased cell permeability leading to augmented intestinal absorption that has been reported in states of sepsis caused by LPS [16]. In cells, the LPS effect was suppressed in the presence of 50  $\mu$ M squalene (Fig. 6a) as it was also observed in animals.

In Caco-2 cells, most of the SGLT1 transporter locates to the intracellular compartments and only a small amount is found in the apical membrane. Khoursandi et al. proposed a possible mechanism of regulation: in their hypothesis, the SGLT1 of the apical membrane would be inactivated after a period of time with respect to the transport capacity of D-glucose and then endocytosed. The endosomal SGLT1, in turn, would eventually be activated and return to the plasma membrane. The entry of D-glucose sodium dependent to the cell

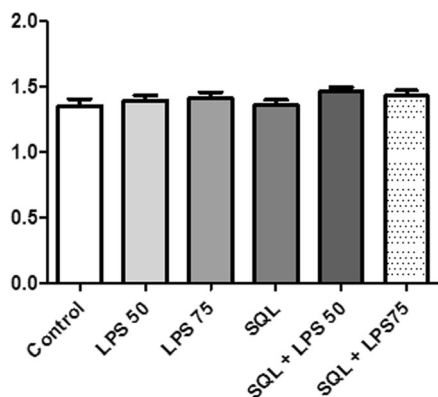


**Fig. 5** Study of the cytotoxicity (MTT) of squalene (SQL) 50  $\mu$ M and LPS at the concentration 50 and 75  $\mu$ g/mL on Caco-2 cells. The results are given as absorbance values. The number of determinations was 12

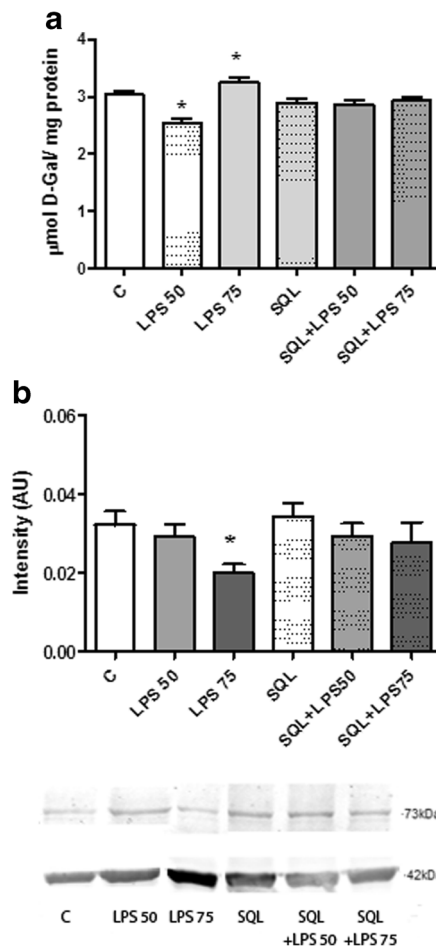


**Fig. 6** Uptake of D-galactose in Caco-2 cells under different conditions. **a** Absorption of 0.5 mM D-galactose in the absence (control) or presence of 50 and 75  $\mu$ g/mL LPS and/or 50  $\mu$ M squalene after 24 h of pre-incubation time. Incubation time with sugar 15 mins.  $N=12$  in each condition. \* $p < 0.05$  with respect to control animals. Protein study by western blot. The information is given as protein expression intensity (mean  $\pm$  SEM) in arbitrary units (AU) normalized to actin expression. **b** SGLT1 expression. \* $p < 0.05$  with respect to control animals

could therefore be regulated without altering the cellular distribution of SGLT1 at steady state, by changes in the speed of the activation/inactivation cycle of SGLT1, which would ultimately determine the amount of transporter in the membrane [19].

Based on the results obtained in D-galactose uptake, we studied by western blot the amount of SGLT1 protein in different cells conditions with/without squalene and/or LPS. The results have shown a significant reduction in the expression of the SGLT1 transporter in the presence of 75  $\mu$ g/mL LPS precisely when absorption was increased (Fig. 6b). The effect of endotoxin was suppressed by squalene. On the other hand, at 50  $\mu$ M LPS, the inhibition observed in the absorption of sugar could be due to an alteration of the intrinsic activity of SGLT1 since the amount of SGLT1 protein was not modified.

In summary, according to the results obtained in the present work, we can propose that LPS at high doses increases the

absorption of D-galactose by an alteration of the paracellular pathway. At the same time, there is a decrease in the active transport of sugar. However, the effect of endotoxin on paracellular way seems to be more important than on the transcellular route. This hypothesis would be supported with the increase in RELM- $\beta$  expression observed which could be the cause of the decrease in SGLT1 levels. In this regard, Krimi et al. showed that RELM- $\beta$  was able to decrease the activity and expression of SGLT1 in the brush border membrane [20].

In addition, the increased absorption of D-galactose by LPS observed may be due to an increase in MLCK protein since this protein is involved in cell permeability via paracellular. Several studies have shown that LPS increases the permeability by tight junctions [16]. The increase in protein expression of MLCK would lead to an increase in MLC phosphorylation that would produce the contraction of the actin-myosin ring, thereby increasing solute transport via paracellular. Likewise, it has been documented that LPS and IL-1 $\beta$  activate MLCK affecting cellular permeability [1].

On the other hand, the effect of low doses of LPS could be related to the intrinsic activity of SGLT1. The activity of this protein can be modified by several factors, among which are proteins like MAPK and PI3K [18]. In this way, our group has shown in previous studies that these kinases were activated by the LPS [4].

## Docking studies

SGLT1 is a membrane glycoprotein localized in the brush border of the intestinal epithelium. The structure of rabbit or human SGLT1 proteins has not been resolved yet. For SGLT1, using Robetta software, one domain spanning amino acids 1 to 662 has been identified as a transmembrane one. This domain was identified as a protein transport and aligned to the structure of the K294A mutant of vSGLT (PDB 2XQ2) [39] (amino acids 1 to 530) with confidence of 0.6752. Within this domain, 5 different models were produced and validated using ProSA-web and ModEval. Validation parameters are shown in Table S1. The predicted root-mean-squared deviation (RMSD) between the coordinates of the C $\alpha$  atoms in the models and in the native structure was below 3 Å in all cases and at least 75% of C $\alpha$  atoms were predicted to be within 3.5 Å of their positions in the native structure. GA341, a score for the reliability of the model, derived from statistical potentials, was higher than a pre-specified cutoff (0.7) in all the cases. This fact indicates that the probability of the correct fold is larger than 95% in all obtained models. We also calculated Z-DOPE and Z-score as parameters of protein model quality. Finally, based on the values obtained for Z-score, RMSD, and Z-DOPE, we selected model 5 for further analysis. For model 5, Ramachandran plot was assessed, revealing that 94.4% of the residues were localized in favored regions,

4.8% were in allowed regions, and only 0.8% of all residues were placed in outlier regions (Fig. S1A).

The structure of rabbit MLCK was also modeled using Robetta. In the first step, five domains were predicted (Table S2). Based on confidence level, ab initio and homology algorithms were used to model domain 1, whereas domains 2 to 5 were modeled by homology. After modeling the five domains, Robetta generated 5 different structures which were validated using ProSA-web and ModEval. Validation parameters are shown in Table S3. For all models, GA341, a score for the reliability of a model, was higher than a pre-specified cutoff (0.7). Predicted RMSD between the coordinates of the C $\alpha$  atoms in the models and in the native structure was above 3 Å in all cases and only in the case of model 2, and at least 75% of C $\alpha$  atoms were predicted to be within 3.5 Å of their positions in the native structure. Finally, based on the values obtained for Z-score, RMSD, and Z-DOPE, we selected model 2 for further analysis. For model 2, Ramachandran plot was assessed, revealing that 94.4% of the residues were localized in favored regions, 4.8% were in allowed regions, and only 0.8% were residues placed in outlier regions (Fig. S1B).

## Docking analysis of SGLT1

Docking between SGLT1 and squalene generated 32 different clusters of docking solutions concentrated in 6 different regions of the protein, while docking between SGLT1 and lipopolysaccharide produced 31 different clusters gathered in 5 different zones of the protein. To facilitate the study, for each region, we selected the element whose interaction with the protein reported the most favorable  $\Delta G$ . In consequence, we reduce the study to the analysis of 6 different ligand positions for the docking of SGLT1 and squalene and 5 different ligand positions for SGLT1 and lipopolysaccharide (Fig. 7).

We used Chimera to analyze the interaction surfaces between the protein and the different docked ligands. We found 4 common interaction areas between lipopolysaccharide and squalene. In those areas, the estimated  $\Delta G$  energy has shown that the interaction between SGLT1 was more favorable than the interaction of SGLT1 with squalene (Table S3). We analyzed the different interactions that could be established between the SGLT1 and both ligands. Clashes and contact analyses did not report any interaction between any of the docked squalene and SGLT1. The same negative result was obtained for the docked lipopolysaccharide and SGLT1. We also used chimera to find possible hydrogen bonds formed. Chimera has shown that all docked lipopolysaccharide could form at least one hydrogen bond with SGLT1, whereas any of the docked squalene reported any possible hydrogen bond formation with SGLT1 (3 and 4). The amino acids involved in these interactions are Lys 342 in interaction zone 2 (zone 1); Arg 52 and Arg 42 in interaction zone 2; Met 512 in interaction zone 3; Arg 259, Arg 564, and Trp 561 in interaction zone 4; and Gln

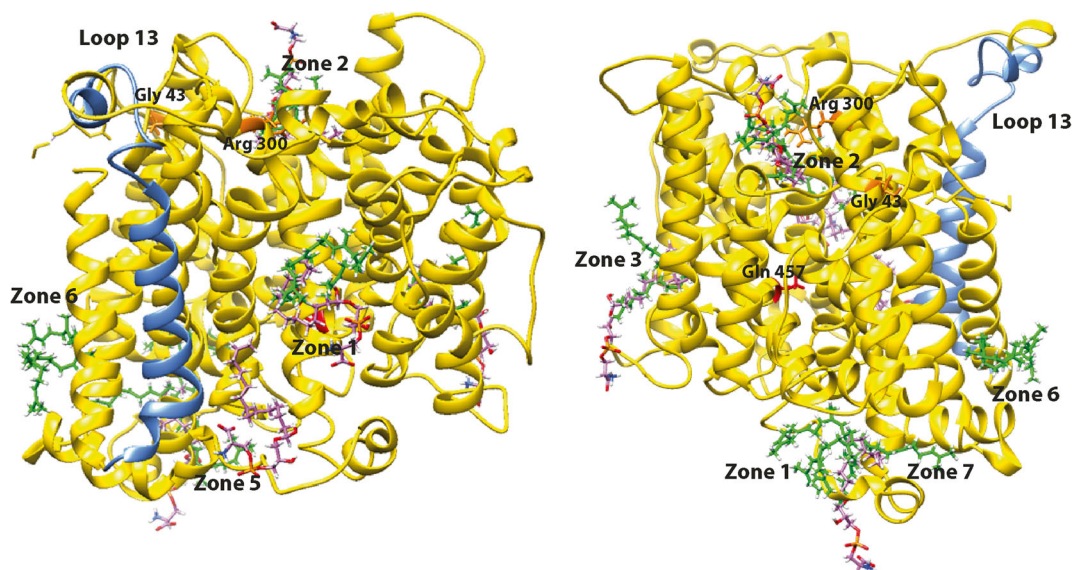


**Fig. 7** Docking analysis. Visualization of the predicted interaction areas between SGLT1 and LPS (purple) and between SGLT1 and squalene (green). We also represented the binding site for glucose (Gln 457) in red, for  $\text{Na}^+$  (Arg 300 and Gly 43) in orange, and for inhibitors (loop 13) in blue

253, Lys 254 in interaction zone 5. This fact explains the higher affinity of LPS for SGLT1. The amino acids involved in these interactions are Lys 342 in interaction zone 2 (zone 1); Arg 52 and Arg 42 in interaction zone 2; Met 512 in interaction zone 3; Arg 259, Arg 564, and Trp 561 in interaction zone 4; and Gln 253, Lys 254 in interaction zone 5. (Figure S2).

SGLT1 functions as an active transporter for glucose. This protein transports one molecule of glucose inside the cells by co-transporting two molecules of  $\text{Na}^+$ . During this process, SGLT1 experiences a series of voltage- and ligand-induced conformational changes. For instance, the interaction of the inhibitor phlorizin with the C-terminal loop 13 of SGLT1 promotes major conformational changes in the protein that affects its activity. On the other hand, interactions that involve the binding site for  $\text{Na}^+$  (Gly 43 and Arg 300) or for glucose (Gln 457) are expected to affect to the function of the protein

(Consortium, 2017). In consequence, we analyze the capacity of LPS and squalene to interact with those regions. We found that both LPS and squalene can bind to SGLT1 in a region close to Arg 300 (interaction zone 2). Moreover, the obtained  $\Delta G$  energy between LPS and SGLT1 in this area was the most favorable one. On the other hand, LPS, but not squalene can interact with the C-terminal loop 13 of SGLT1 although the affinity is lower than for interaction zone 2 (Fig. S2).

#### Docking analysis of MLCK

Docking experiments were carried out with RossieLigand using model 2 MLCK structure as a template and the ligand ZINC06845904 (squalene) and ZINC38377593 (lipopolysaccharide).

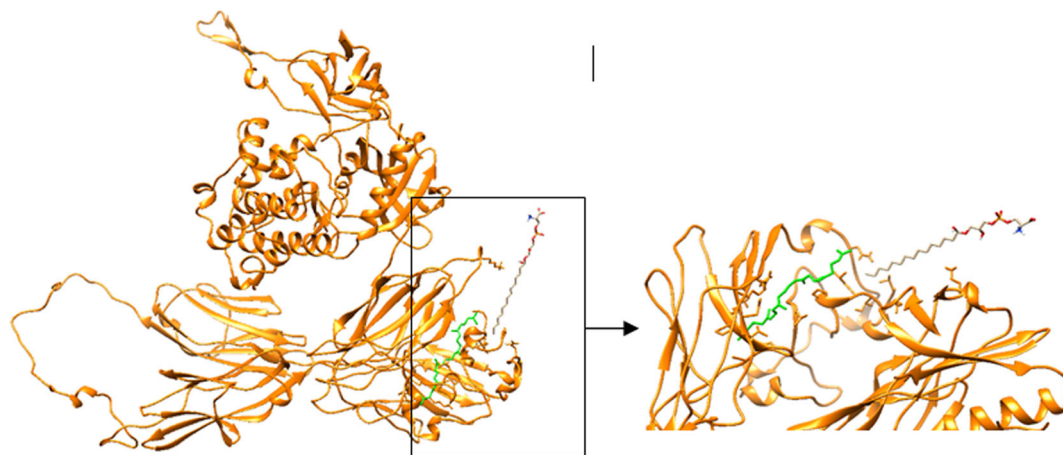


**Fig. 8** Analysis of the four interaction zones of MLCK with lipopolysaccharide (in gray) and squalene (in green)

Solutions of docking MLCK-lipopolysaccharide and docking MLCK-squalene were concentrated in just one region of the protein. Comparing both dockings, both ligands share a common interaction. In this area, the estimated  $\Delta G$  energy has shown that the interaction between MLCK and lipopolysaccharide was more favorable than the interaction of MLCK with squalene (Table S4).

Interaction surfaces between the protein and the different docked ligands were analyzed using Chimera. Clashes and contact analyses did not report any interaction between any of the docked squalene and MLCK. The same negative result was obtained for the docked lipopolysaccharide and MLCK. We also used Chimera to find possible hydrogen bonds formed between MLCK and both ligands. Chimera has shown that all docked lipopolysaccharide could form at least one hydrogen bond with MLCK, whereas any of the docked squalene reported any possible hydrogen bond formation with MLCK (Fig. 8).

In both cases, the amino acids that could be involved in the binding between the protein and the ligands are Val 116, Glu 133, Thr 124, Leu 125, Lys 126, Ile 221, Asn 223, Lys 658, and Glu 660. Most of the amino acids involved in the binding area are placed in the actin-binding domain, whereas the proton acceptor of the active center (Asp 817) and the amino acids involved in the ATP binding (Lys 125) seem not to be involved in the binding zone.

In addition, the results obtained by bioinformatic analysis indicate a possible interaction between squalene and LPS with the binding site for  $\text{Na}^+$  of the SGLT1 transporter, which modified its intrinsic activity. Perhaps, it seems that in the case of LPS, a slight interaction could be given, which added to the aforementioned by the action of the kinases, and could modify the affinity of the transporter for sugar, a fact that could occur in the case of low doses or concentrations of endotoxin.

Likewise, bioinformatic studies have shown an area of interaction between SGLT1 and RELM- $\beta$  that could affect the transporter.

On the other hand, it was observed that the sugar absorption in the group with LPS but fed the diet supplemented with 0.5% squalene was not increased.

Through bioinformatic studies, it was observed that squalene could interact with the active site of MLCK and this event could affect the functionality of the kinase. But in what way does squalene cancel the effect of LPS?

Previous studies carried out by our group on rabbits and Caco-2 cells have shown that LPS, TNF- $\alpha$ , and IL-1 $\beta$  inhibit the intestinal absorption of D-galactose by modifying the activity or capacity of transport of SGLT1 through the activation of intracellular pathways in which kinase proteins are involved, such as PKC, PI3K, MAPK's, and nuclear transcription factor (NF-kB) [3–5, 36, 37].

In addition, several studies relate the anti-inflammatory effect of the hydrocarbon polyphenols (squalene),  $\beta$ -carotenes,

etc. of virgin olive oil with the inactivation of NF-kB [26]. Therefore, maybe squalene could cancel the effect of LPS by inactivating NF-kB, but future studies in this regard should be done.

In summary, squalene could reverse the effect of LPS through its interaction with MLCK and NF-kB. In addition, bioinformatic studies confirm the interaction between LPS-squalene through the MLCK and SGLT1 proteins.

**Acknowledgments** Molecular graphics and analyses were performed with the UCSF Chimera package. Chimera is developed by the Resource for Biocomputing, Visualization, and Informatics at the University of California, San Francisco (supported by NIGMS P41-GM103311).

**Funding information** This work was supported by grants from Grants from Ministerio de Economía y Competitividad, Gobierno de España (SAF2016-75441-R), CIBERobn (CB06/03/1012), Gobierno de Aragón (B16-R17), and SUDOE (Redvalue, SOE1/PI/E0123).

## Compliance with ethical standards

All experimental protocols were approved by the Ethical Committee of the University of Zaragoza (PI47/10).

**Conflict of interest** The authors declare that they have no conflict of interests.

## References

1. Al-Sadi R, Guo S, Dokladny K, Smith MA, Ye D, Kaza A, Watterson DM, Ma TY (2012) Mechanism of interleukin-1 $\beta$  induced-increase in mouse intestinal permeability in vivo. *J Interf Cytokine Res* 32:474–484. <https://doi.org/10.1089/jir.2012.0031>
2. Al-Sadi R, Guo S, Ye D, Rawat M, Ma TY (2016) TNF- $\alpha$  modulation of intestinal tight junction permeability is mediated by NIK/IKK- $\alpha$  axis activation of the canonical NF- $\kappa$ B pathway. *Am J Pathol* 186:1151–1165. <https://doi.org/10.1016/j.ajpath.2015.12.016>
3. Amador P, Garcia-Herrera J, Marca MC, de la Osada J, Acin S, Navarro MA, Salvador MT, Lostao MP, Rodriguez-Yoldi MJ (2007) Inhibitory effect of TNF- $\alpha$  on the intestinal absorption of galactose. *J Cell Biochem* 101:99–111. <https://doi.org/10.1002/jcb.21168>
4. Amador P, Garcia-Herrera J, Marca MC, de la Osada J, Acin S, Navarro MA, Salvador MT, Lostao MP, Rodriguez-Yoldi MJ (2007) Intestinal D-galactose transport in an endotoxemia model in the rabbit. *J Membr Biol* 215:125–133. <https://doi.org/10.1007/s00232-007-9012-5>
5. Amador P, Marca MC, Garcia-Herrera J, Lostao MP, Guillen N, de la Osada J, Rodriguez-Yoldi MJ (2008) Lipopolysaccharide induces inhibition of galactose intestinal transport in rabbits in vitro. *Cell Physiol Biochem* 22:715–724. <https://doi.org/10.1159/000185555>
6. Berkes J, Viswanathan VK, Savkovic SD, Hecht G (2003) Intestinal epithelial responses to enteric pathogens: effects on the tight junction barrier, ion transport, and inflammation. *Gut* 52:439–451
7. Cardeno A, Magnusson MK, Strid H, Alarcon de La Lastra C, Sanchez-Hidalgo M, Ohman L (2014) The unsaponifiable fraction

- of extra virgin olive oil promotes apoptosis and attenuates activation and homing properties of T cells from patients with inflammatory bowel disease. *Food Chem* 161:353–360. <https://doi.org/10.1016/j.foodchem.2014.04.016>
8. Clayburgh DR, Rosen S, Witkowski ED, Wang F, Blair S, Dudek S, Garcia JG, Alverdy JC, Turner JR (2004) A differentiation-dependent splice variant of myosin light chain kinase, MLCK1, regulates epithelial tight junction permeability. *J Biol Chem* 279:55506–55513. <https://doi.org/10.1074/jbc.M408822200>
  9. Chantret I, Rodolosse A, Barbat A, Dussaulx E, Brot-Laroche E, Zweibaum A, Rousset M (1994) Differential expression of sucrase-isomaltase in clones isolated from early and late passages of the cell line Caco-2: evidence for glucose-dependent negative regulation. *J Cell Sci* 107(Pt 1):213–225
  10. Choudhry N, Bajaj-Elliott M, McDonald V (2008) The terminal sialic acid of glycoconjugates on the surface of intestinal epithelial cells activates excystation of *Cryptosporidium parvum*. *Infect Immun* 76:3735–3741. <https://doi.org/10.1128/IAI.00362-08>
  11. Dawson DJ, Burrows PC, Loble RW, Holmes R (1987) The kinetics of monosaccharide absorption by human jejunal biopsies: evidence for active and passive processes. *Digestion* 38:124–132. <https://doi.org/10.1159/000199581>
  12. DeLuca S, Khar K, Meiler J (2015) Fully flexible docking of medium sized ligand libraries with RosettaLigand. *PLoS One* 10:e0132508. <https://doi.org/10.1371/journal.pone.0132508>
  13. Ferraris RP, Diamond J (1997) Regulation of intestinal sugar transport. *Physiol Rev* 77:257–302. <https://doi.org/10.1152/physrev.1997.77.1.257>
  14. Garcia-Barrios A, Guillen N, Gascon S, Osada J, Vazquez CM, Miguel-Carrasco JL, Rodriguez-Yoldi MJ (2010) Nitric oxide involved in the IL-1beta-induced inhibition of fructose intestinal transport. *J Cell Biochem* 111:1321–1329. <https://doi.org/10.1002/jcb.22859>
  15. Grosdidier A, Zoete V, Michielin O (2011) Fast docking using the CHARMM force field with EADock DSS. *J Comput Chem* 32:2149–2159. <https://doi.org/10.1002/jcc.21797>
  16. Guo S, Al-Sadi R, Said HM, Ma TY (2012) Lipopolysaccharide causes an increase in intestinal tight junction permeability in vitro and in vivo by inducing enterocyte membrane expression and localization of TLR-4 and CD14. *Am J Pathol* 182:375–387. <https://doi.org/10.1016/j.ajpath.2012.10.014>
  17. Hecht G, Koutsouris A (1999) Enteropathogenic *E. coli* attenuates secretagogue-induced net intestinal ion transport but not Cl<sup>-</sup> secretion. *Am J Phys* 276:G781–G788
  18. Helliwell PA, Richardson M, Affleck J, Kellett GL (2000) Regulation of GLUT5, GLUT2 and intestinal brush-border fructose absorption by the extracellular signal-regulated kinase, p38 mitogen-activated kinase and phosphatidylinositol 3-kinase intracellular signalling pathways: implications for adaptation to diabetes. *Biochem J* 350(Pt 1):163–169
  19. Khoursandi S, Scharlau D, Herter P, Kuhnen C, Martin D, Kinne RK, Kipp H (2004) Different modes of sodium-D-glucose cotransporter-mediated D-glucose uptake regulation in Caco-2 cells. *Am J Physiol Cell Physiol* 287:C1041–C1047. <https://doi.org/10.1152/ajpcell.00197.2004>
  20. Krimi RB, Letteron P, Chedid P, Nazaret C, Ducroc R, Marie JC (2009) Resistin-like molecule-beta inhibits SGLT-1 activity and enhances GLUT2-dependent jejunal glucose transport. *Diabetes* 58:2032–2038. <https://doi.org/10.2337/db08-1786>
  21. Lou-Bonafonte JM, Martinez-Beamonte R, Sanclemente T, Surra JC, Herrera-Marcos LV, Sanchez-Marco J, Amal C, Osada J (2018) Current insights into the biological action of squalene. *Mol Nutr Food Res* 62:e1800136. <https://doi.org/10.1002/mnfr.201800136>
  22. Ma TY, Anderson JM (2012) Tight Junctions and the intestinal barrier. Inc: *Physiology of the Gastrointestinal Tract*. Elsevier Academic Press, Burlington, MA
  23. Nighot M, Al-Sadi R, Guo S, Rawat M, Nighot P, Watterson MD, Ma TY (2017) Lipopolysaccharide-induced increase in intestinal epithelial tight permeability is mediated by toll-like receptor 4/myeloid differentiation primary response 88 (MyD88) activation of myosin light chain kinase expression. *Am J Pathol* 187:2698–2710. <https://doi.org/10.1016/j.ajpath.2017.08.005>
  24. Pettersen EF, Goddard TD, Huang CC, Couch GS, Greenblatt DM, Meng EC, Ferrin TE (2004) UCSF chimera—a visualization system for exploratory research and analysis. *J Comput Chem* 25:1605–1612. <https://doi.org/10.1002/jcc.20084>
  25. Reboredo-Rodriguez P, Varela-Lopez A, Forbes-Hernandez TY, Gasparrini M, Afrin S, Cianciosi D, Zhang J, Manna PP, Bompadre S, Quiles JL, Battino M, Giampieri F (2018) Phenolic compounds isolated from olive oil as nutraceutical tools for the prevention and management of cancer and cardiovascular diseases. *Int J Mol Sci* 19. <https://doi.org/10.3390/ijms19082305>
  26. Sanchez-Fidalgo S, Villegas I, Aparicio-Soto M, Cardeno A, Rosillo MA, Gonzalez-Benjumea A, Maset A, Lopez O, Maya I, Fernandez-Bolanos JG, Alarcon de la Lastra C (2015) Effects of dietary virgin olive oil polyphenols: hydroxytyrosyl acetate and 3, 4-dihydroxyphenylglycol on DSS-induced acute colitis in mice. *J Nutr Biochem* 26:513–520. <https://doi.org/10.1016/j.jnutbio.2014.12.001>
  27. Sanchez-Fidalgo S, Villegas I, Rosillo MA, Aparicio-Soto M, de la Lastra CA (2014) Dietary squalene supplementation improves DSS-induced acute colitis by downregulating p38 MAPK and NFkB signaling pathways. *Mol Nutr Food Res* 59:284–292. <https://doi.org/10.1002/mnfr.201400518>
  28. Shirazi-Beechey SP (1995) Molecular biology of intestinal glucose transport. *Nutr Res Rev* 8:27–41. <https://doi.org/10.1079/NRR19950005>
  29. Simons KT, Kooperberg C, Huang E, Baker D (1997) Assembly of protein tertiary structures from fragments with similar local sequences using simulated annealing and Bayesian scoring functions. *J Mol Biol* 268:209–225. <https://doi.org/10.1006/jmbi.1997.0959>
  30. Song Y, DiMaio F, Wang RY, Kim D, Miles C, Brunette T, Thompson J, Baker D (2013) High-resolution comparative modeling with RosettaCM. *Structure* 21:1735–1742. <https://doi.org/10.1016/j.str.2013.08.005>
  31. Tsukita S, Furuse M, Itoh M (2001) Multifunctional strands in tight junctions. *Nat Rev Mol Cell Biol* 2:285–293. <https://doi.org/10.1038/35067088>
  32. Turner JR (2009) Intestinal mucosal barrier function in health and disease. *Nat Rev Immunol* 9:799–809. <https://doi.org/10.1038/nri2653>
  33. van Meerloo J, Kaspers GJ, Cloos J (2011) Cell sensitivity assays: the MTT assay. *Methods Mol Biol* 731:237–245. [https://doi.org/10.1007/978-1-61779-080-5\\_20](https://doi.org/10.1007/978-1-61779-080-5_20)
  34. Vayro S, Wood IS, Dyer J, Shirazi-Beechey SP (2001) Transcriptional regulation of the ovine intestinal Na<sup>+</sup>/glucose cotransporter SGLT1 gene. Role of HNF-1 in glucose activation of promoter function. *Eur J Biochem* 268:5460–5470
  35. Veyhl M, Keller T, Gorboulev V, Vernalen A, Koepsell H (2006) RS1 (RSC1A1) regulates the exocytotic pathway of Na<sup>+</sup>–D-glucose cotransporter SGLT1. *Am J Physiol Renal Physiol* 291:F1213–F1223. <https://doi.org/10.1152/ajprenal.00068.2006>
  36. Vinales C, Gascon S, Barranquero C, Osada J, Rodriguez-Yoldi MJ (2012) Inhibitory effect of IL-1beta on galactose intestinal absorption in rabbits. *Cell Physiol Biochem* 30:173–186. <https://doi.org/10.1159/000339056>
  37. Vinales C, Gascon S, Barranquero C, Osada J, Rodriguez-Yoldi MJ (2013) Interleukin-1beta reduces galactose transport in intestinal epithelial cells in a NF-kB and protein kinase C-dependent manner. *Vet Immunol Immunopathol* 155:171–181. <https://doi.org/10.1016/j.vetimm.2013.06.016>

38. Warleta F, Campos M, Allouche Y, Sanchez-Quesada C, Ruiz-Mora J, Beltran G, Gaforio JJ (2010) Squalene protects against oxidative DNA damage in MCF10A human mammary epithelial cells but not in MCF7 and MDA-MB-231 human breast cancer cells. *Food Chem Toxicol* 48:1092–1100. <https://doi.org/10.1016/j.fct.2010.01.031>
39. Watanabe A, Choe S, Chaptal V, Rosenberg JM, Wright EM, Grabe M, Abramson J (2010) The mechanism of sodium and substrate release from the binding pocket of vSGLT. *Nature* 468:988–991. <https://doi.org/10.1038/nature09580>
40. Wiederstein M, Sippl MJ (2007) ProSA-web: interactive web service for the recognition of errors in three-dimensional structures of proteins. *Nucleic Acids Res* 35:W407–W410. <https://doi.org/10.1093/nar/gkm290>
41. Xu J, Liu Z, Zhan W, Jiang R, Yang C, Zhan H, Xiong Y (2018) Recombinant TsP53 modulates intestinal epithelial barrier integrity via upregulation of ZO1 in LPS-induced septic mice. *Mol Med Rep* 17:1212–1218. <https://doi.org/10.3892/mmr.2017.7946>
42. Yu LC, Turner JR, Buret AG (2006) LPS/CD14 activation triggers SGLT-1-mediated glucose uptake and cell rescue in intestinal epithelial cells via early apoptotic signals upstream of caspase-3. *Exp Cell Res* 312:3276–3286. <https://doi.org/10.1016/j.yexcr.2006.06.023>

**Publisher's note** Springer Nature remains neutral with regard to jurisdictional claims in published maps and institutional affiliations.